Gold Catalysts

DOI: 10.1002/anie.201301383

Resonant Photoemission Observations and DFT Study of s–d Hybridization in Catalytically Active Gold Clusters on Ceria Nanorods**

*Yunyun Zhou, Neil J. Lawrence, Lu Wang, Lingmei Kong, Tai-Sing Wu, Jing Liu, Yi Gao, Joseph R. Brewer, Vivianna K. Lawrence, Renat F. Sabirianov, Yun-Liang Soo, Xiao Cheng Zeng, Peter A. Dowben, Wai Ning Mei, and Chin Li Cheung**

Gold clusters have garnered intense interest because of their catalytic activities towards chemical reactions of industrial and environmental importance.[1] The most investigated chemical reactions on gold clusters are those involving molecular oxygen (O_2). Activation (adsorption and dissociation) of the O_2 molecules on the gold surface is a key limiting factor in the catalytic processes because of the thermodynamically unfavorable formation of the chemisorbed O_2^- intermediate.[2] Much research has studied the effects of quantum confinement,[3] cluster geometry,[2] and charge transfer[4] to illustrate the enhanced catalytic activity of metal oxide supported gold systems for carbon monoxide (CO) oxidation. The electronic structure of oxide supported gold clusters can provide critical clues to the mechanisms for their catalytic activity and descriptions of the valence band structure and may explain the electronic origin in these catalyzed reactions.[5] Gold atoms have an electronic configuration of $[Xe]4f^{14}5d^{10}6s^1$. The relativistic effects in gold, however, stabilize its 6s orbital and destabilize its 5d orbitals.[6] Thus, for gold clusters, these effects, together with upward shift of the 5d orbitals to the Fermi level, lead to a decrease in the s–d energy gap and hence allow the theoretically expected hybridization of the 5d and 6s orbitals.[6a,7] These s–d hybridized orbitals (or bands) essentially increase the number of free d states (number of d holes) available for bonding with incoming reactant molecules and lowering the transition state energy to promote the reactions.[4b] Though the importance of the valence band hybridization in gold-cluster-based catalysts has been long postulated, this electronic structure has yet to be observed in active, supported gold cluster catalyst systems.

In this study, we investigated s–d hybridization in catalytically active gold clusters supported on ceria nanorods (0.01 at.% Au:CeO_{2-x}), by applying resonant photoemission spectroscopy (RPES). The RPES results establish the existence of a 5d-hole population in these gold clusters through the observation of resonant enhancements for the 5p-to-5d and 4f-to-5d electronic transitions. Owing to the strong interactions between the oxygen atoms and gold clusters in low gold concentration systems,[8] we are able to study the 5p-to-5d and 4f-to-5d transitions of the gold clusters indirectly by examining the photoemission of the O 2p derived states. Density functional theory (DFT) calculations were performed on two ceria slab supported gold cluster models to elucidate the detailed 5d and 6s weighted band structure and provide theoretical support to both validate and delve into the origin of the hybridization between these bands in low gold concentration Au:CeO_{2-x} catalysts.

Catalytically active 0.01 at.% Au:CeO_{2-x} nanorods were prepared by a wet impregnation method to deposit gold clusters onto ceria nanorods using a modified hydrothermal method.[9] Detailed morphology and concentration characterizations are in the Supporting Information. Extended X-ray absorption fine structure (EXAFS) analysis of the Ce-L_3 edge absorption spectrum of the sample indicated the presence of a high density of oxygen vacancy sites in the ceria nanorods as suggested by the low coordination number (CN = 6.6) of Ce-O in first shell when compared to that of the perfect CeO_2 structure (CN = 8). Our low gold concentration Au:CeO_{2-x} sample has a high catalytic activity towards the oxidation of CO with a light-off temperature (T_{50}, 50% CO conversion) at approximately 100 °C, while that of ceria nanorods (CeO_{2-x}) is at approximately 200 °C (see Supporting Information).

The local structure of the gold clusters in the 0.01 at.% Au:CeO_{2-x} nanorods was studied using X-ray absorption near

[*] Y. Zhou, N. J. Lawrence, Dr. Y. Gao, Dr. J. R. Brewer, V. K. Lawrence, Prof. Dr. X. C. Zeng, Prof. Dr. C. L. Cheung
Department of Chemistry, University of Nebraska-Lincoln
Lincoln, NE 68588 (USA)
E-mail: ccheung2@unl.edu
Dr. L. Kong, Dr. J. Liu, Prof. Dr. P. A. Dowben
Department of Physics and Astronomy, University of Nebraska-Lincoln
Lincoln, NE 68588 (USA)
Dr. L. Wang, Prof. Dr. R. F. Sabirianov, Prof. Dr. W. N. Mei
Department of Physics, University of Nebraska at Omaha
Omaha, NE 68182 (USA)
T.-S. Wu, Prof. Dr. Y.-L. Soo
Department of Physics, National Tsing Hua University
National Synchrotron Radiation Research Center (Taiwan)

[**] This research was supported by Nebraska Center for Energy Sciences, National Science Foundation through Nebraska MRSEC (DMR-0820521), Nebraska Center for Materials and Nanoscience (DMR-0960110) and NSF-EPSCoR program (EPS-1010674), Department of Energy (DE-EE0003174), and Army Research Office (W911NF-10-2-0099). The University of Nebraska Holland Computing Center has provided computations resources. We thank the University of North Texas and Center for Advanced Microstructures & Devices for the use of their facilities. We are grateful to Dr. David Diercks and Dr. Yaroslav Losovyj for their help with microscopy and spectroscopy experiments.

Supporting information for this article is available on the WWW under http://dx.doi.org/10.1002/anie.201301383.

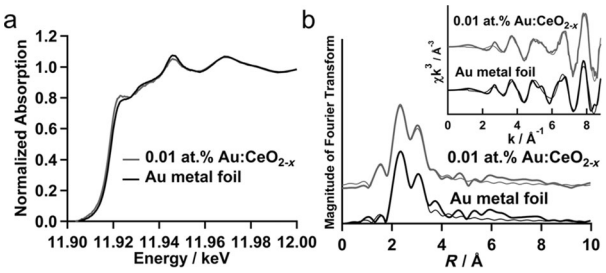

Figure 1. a) Normalized Au L_3-edge XANES spectra of 0.01 at.% Au:CeO_{2-x} nanorods and the reference gold metal foil. b) Fourier transformed Au L_3-edge EXAFS data in (a). The inset data are the corresponding EXAFS functions in *k* space. (Thick lines: data; thin lines: fittings, spectra vertically offset for clarity.)

edge structure (XANES). Figure 1a shows the normalized Au L_3-edge XANES data of the catalyst and a gold metal foil. The absorption spectrum from the gold clusters in the catalyst exhibits similar features to that of the reference gold metal foil, except that the spectrum for the catalyst has a more intense white line (a feature at the top of the sharply rising part of spectrum at ca. 11.92 keV). Since the intensity of the resonance at the threshold (white line) is associated with a $2p_{3/2}$-to-$5d_{5/2,3/2}$ dipole transition, the more intense white line indirectly suggests an increase in the d-hole population in the gold clusters of the Au:CeO_{2-x} catalyst.[10]

EXAFS data in Figure 1b demonstrates the presence of metal–substrate bonds in the Fourier transformed spectrum for the 0.01 at.% Au:CeO_{2-x} because of an increase in density of states in the radial distribution function at very low radii. In general, it should be noted that the spectra of the oxide supported clusters look similar to that of the gold foil. This metal–substrate bond can be attributed to a Au–O bond with an average length of 2.02 Å (Table SI-1), indicating a strong interaction between the gold clusters and their ceria supports.[8a] A slightly shorter Au–Au atomic distance (2.83 Å) and lower coordination number (CN = 8.9) were observed in the catalyst than those of the reference gold metal foil. (Table SI-1) The shorter average Au–Au bond length indicates the small gold cluster sizes in the catalyst. This small size effect which has been proposed to increase the d-hole population in gold clusters[10] is also supported by the more intense white line observed in the Au XANES data.

The electronic structure and valence band spectra (VBS) of the 0.01 at.% Au:CeO_{2-x} were investigated using RPES to determine if resonant enhancements of the valence band electronic transitions occur for the gold clusters at photon energies corresponding to the gold 5p and 4f threshold, an indication of both 5p-to-5d and 4f-to-5d transitions. The existence of such resonances is a direct evidence for the existence of 6s–5d hybridization. The photoelectron spectra were acquired at different photon energies from 65 to 105 eV for the RPES of the O 2p states from the ceria support. Owing to the strong interactions between gold clusters and the ceria support,[8b,11] we focused on investigating the O 2p derived states to elucidate the gold resonance in the catalyst sample and confirm the existence of strong gold interaction with the catalyst support (ceria nanorods).

Figure 2a shows the normalized intensity of the VBS recorded at different incident photon energies. (Binding energies are denoted in terms of $E-E_F$.) In Figure 2b it is replotted and interpolated using false color in a two-dimensional manner to demonstrate the intensity change of photoemission corresponding to the photon energy variation. To evaluate the electronic properties and contributions of different bonding and nonbonding orbitals to the VBS, three

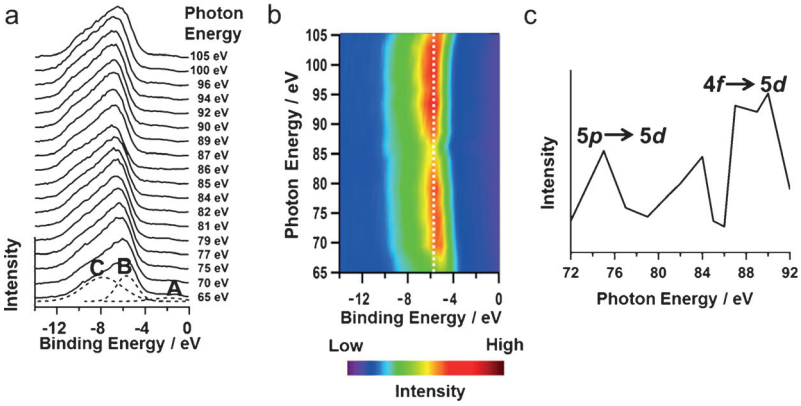

Figure 2. a) Fitted valence band resonant photoemission spectra for the 0.01 at.% Au:CeO_{2-x} nanorods taken at photon energies in the range of 65–105 eV. b) Interpolated 2D false color plot using data in (a). White dashed line: Binding energy at −5.7 eV. c) Plot of photoemission intensities at −5.7 eV binding energy as a function of photon energy for the Au in Au:CeO_{2-x} using the fitting data for Peak B. Binding energies are denoted in terms of $E-E_F$.

Gaussian peaks were fitted to model the RPES spectra in Figure 2a. These spectra consist of a peak appearing at a binding energy of approximately −2 eV (labeled as Peak A) and a broad band stretching from −10 eV to −4 eV (Peaks B and C), which correspond to the primarily O 2p derived states of the ceria support.[12] Peak A is attributed to the emission of electrons from the localized Au 5d state, whose weak intensity is due to the low loading of gold on the catalyst surface. The valence band state enhancement for our catalyst is broadened, between −8 eV and −2 eV, in the resonant photoemission spectra, while that of bulk gold is from −6 eV to −3 eV.[13] This broadening of the valence band features, a typical feature for small-sized gold clusters, is the result of increased inhomogeneity of gold atoms in the clusters and the presence of more localized unoccupied d states at the Fermi level.[10] The changes in the valence spectral density is consistent with the Au L_3-edge XANES data that indicates an increase in the d-hole population in the gold clusters of Au:CeO_{2-x}. In Figure 2, Peaks B and C in the broad band (−10 eV to −4 eV binding energy) arise from the photoemission from the O $2p_x$, O $2p_y$ orbitals (−5.7 eV binding energy) and O $2p_z$ orbital (−7.7 eV binding energy), respec-

tively.[14] The photoemission originating from Au 5d band is expected to yield an emission at around −6 to −4 eV binding energy or in the region of these peaks but closer to the Fermi level in the smaller gold clusters.

Although it is difficult to identify photoemission originating strictly from Au 5d band, owing to the trace amount of gold in our catalyst, the resonant enhancement of the valence band in the photoemission from gold clusters can be clearly observed in the plot of the intensities of Peak B as a function of photon energy at the Au 5p and 4f thresholds (Figure 2b). The maximum intensities in the photoemission spectra occur at roughly Au $5p_{1/2}$ (74.2 eV) and $4f_{5/2}$ (87.6 eV) core threshold binding energies, and are indicative of the $5p_{1/2}$-to-$5d_{3/2}$ and $4f_{5/2}$-to-$5d_{3/2}$ transitions of bulk gold, respectively.[15] Since the electronic configuration of a gold atom ($[Xe]4f^{14}5d^{10}6s^1$) indicates a full 5d subshell, these transitions can only occur if there is partial, not complete, occupancy of the valence Au 5d band. This d-hole population deduced from the RPES data is ascribed to the hybridization of 5d and 6s states in the gold clusters.

The existence of s–d hybridization in the Au:CeO_{2-x} catalyst is also predicted in our density functional theory (DFT) models composed of gold clusters on cerium oxide slabs. A 19-atom-layered Au(111) slab model was used to simulate the electronic structure of bulk gold. Two different structures of gold clusters composed of 19 gold atoms, tetrahedral Au_{19} (t-Au_{19}; the most stable Au_{19} cluster)[16] and planar Au_{19} (p-Au_{19}; strongly favored by relativistic effect),[17] were considered to represent two extreme cases of Au_{19}:CeO_{2-x} models.

The 6s–5d hybridization in the Au_{19} clusters of the two Au_{19}:CeO_{2-x} models and their catalytic potential were revealed in the computed total and partial density of states (DOS) of these systems. The optimized structure of the t-Au_{19}:CeO_{2-x} model shown in Figure 3 was found to be slightly negatively charged ($-3.21\,e^-$ or $-0.17\,e^-$ per gold atom) from Bader charge analysis. Our results agree well with the previous study of Au_{18} on a MgO film ($-3.54\,e^-$ and $-0.2\,e^-$ per gold atom).[18] The excess charge in the t-Au_{19} cluster is probably derived from the electron density of the oxygen vacancies in the defective ceria slab support.[8b] Comparisons between the total density of states of the CeO_{2-x} slab, t-Au_{19}, and t-Au_{19}:CeO_{2-x} in Figure 3c and Figure SI-4 suggest that the interaction of t-Au_{19} with the ceria support possibly introduces the pin-in gap state feature (or metal-induced gap states (MIGS)) present below the empty Ce 4f states and the Fermi level. By analyzing the partial density of states (PDOS) of t-Au_{19}:CeO_{2-x} (Figure 3d), we find that these MIGS are mainly composed of Au 5d and 6s states, consistent with our photoemission findings. The similarities among the shapes of these 5d and 6s band structures in the MIGS region further confirm the strong s–d hybridization in this supported t-Au_{19} cluster. A larger d-hole population is also evident in the PDOS of t-Au_{19}:CeO_{2-x} when compared with that for the Au(111) slab in Figure 3d. Similar s–d hybridization and d-hole population features were also observed in the band structure of the p-Au_{19}:CeO_{2-x} model (Figure SI-4 and -5).

The location of the d-band center with respect to the Fermi level of a transition-metal-based catalyst has been proposed to strongly influence its catalytic activity.[5] The up-shift of the d-band center towards the Fermi level will enhance the formation of chemical bonds between the catalyst and reactant because of the increased availability of symmetry-allowed and energetically favored electronic states from the d band. In our catalyst, the Au 5d band center locations with respect to vacuum level for the isolated t-Au_{19} and t-Au_{19}:CeO_{2-x} are −7.76 and −7.45 eV, respectively. These up-shifted values are in contrast to the energy of −8.85 eV for the Au 5d band center location for the Au(111) slab. This offers a possible explanation for the observed high catalytic behavior of our Au:CeO_{2-x} catalyst for CO oxidation at low temperatures. The t-Au_{19} cluster exhibits a stronger s–d hybridization and up-shift of the d-band center than the Au slab. This s–d hybridization can promote the electron transfer necessary for bonding and back-bonding between the supported Au clusters and O_2 molecules. Similar results are obtained from the p-Au_{19} cluster (Figure SI-5).

Our results for the Au_{19}:CeO_{2-x} model suggest a non-zero transfer of electrons from the defective ceria to the Au_{19} cluster. Such a negative charge transfer has also been predicted to increase the availability of valence electron density of gold for bonding to chemisorbed molecules and affect the strength of highly directional s–d hybridized orbitals.[4b,8b] In the case of oxygen, negatively charged gold clusters can provide more electrons to transfer to π* orbitals

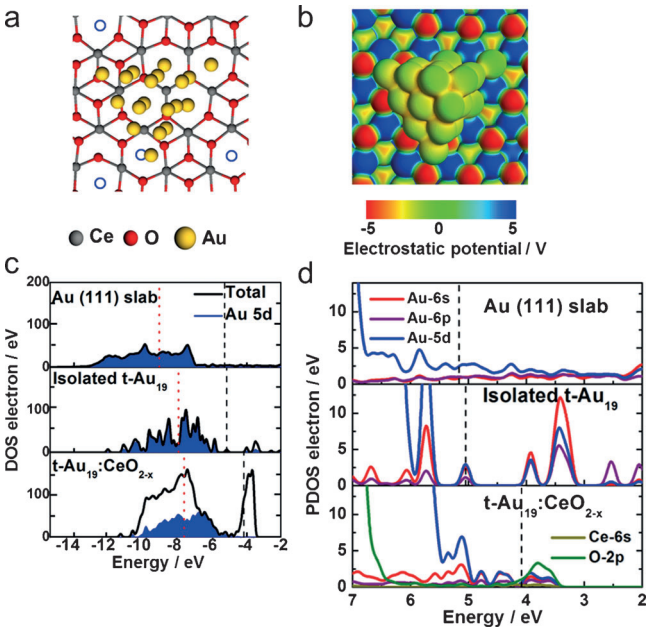

Figure 3. a) Top view of a DFT-optimized structure of a t-Au_{19} cluster adsorbed on a defective 9-atom-thick ceria(111) slab (CeO_{2-x}). Blue circles: oxygen vacancy sites. b) Calculated charge distribution of the t-Au_{19}:CeO_{2-x} model in (a). c) Black: Total surface density of states. Blue: density of states of Au 5d band for top: a 19-atom-thick Au(111) slab, middle: isolated t-Au_{19}, and bottom: t-Au_{19}:CeO_{2-x}. d) Partial density of states (PDOS) for the 6s, 6p, and 5d orbitals of Au in top: Au(111) slab, middle: isolated t-Au_{19}, and bottom: t-Au_{19}:CeO_{2-x}. 6s orbital of Ce and 2p orbital of O in t-Au_{19}:CeO_{2-x} are in the bottom figure. Red dash lines: Au 5d band centers. Black dash lines: Fermi levels with respect to vacuum at $E = 0$ eV.

of the O_2 molecules, which again affects the adsorption energy and dissociation of O_2, leading to higher catalytic activity for CO oxidation. Our computational models also indicate the d-band center up-shifts in small gold clusters, a larger d-hole population in the Au 5d band of our catalyst, and the resulting hybridized s–d orbitals found in our experiment.

In summary, the existence of s–d hybridization in gold clusters of a catalytically active 0.01 at.% $Au:CeO_{2-x}$ catalyst was demonstrated using resonant photoemission spectroscopy and model calculations. Significant $5p_{1/2}$-to-$5d_{3/2}$ and $4f_{5/2}$-to-$5d_{3/2}$ resonant electronic transitions observed in our $Au:CeO_{2-x}$ catalysts indicate the presence of an unfilled 5d subshell (or 5d holes) in the gold clusters of the catalyst and thus provide the evidence for the s–d hybridization. Our approach to investigating the electronic structures of supported low concentration gold catalysts illustrates an alternate pathway to investigate other metal oxide supported metal systems and gain further insights into their structure–reactivity relationship.

Received: February 17, 2013
Published online: May 28, 2013

Keywords: cerium oxide · gold catalysts · hybridization · resonant photoemission spectroscopy

[1] a) M. Chen, D. W. Goodman, *Acc. Chem. Res.* **2006**, *39*, 739 – 746; b) W. Deng, M. Flytzani-Stephanopoulos, *Angew. Chem.* **2006**, *118*, 2343 – 2347; *Angew. Chem. Int. Ed.* **2006**, *45*, 2285 – 2289.

[2] G. Mills, M. S. Gordon, H. Metiu, *J. Chem. Phys.* **2003**, *118*, 4198 – 4205.

[3] a) C. Lemire, R. Meyer, S. Shaikhutdinov, H.-J. Freund, *Angew. Chem.* **2004**, *116*, 121 – 124; *Angew. Chem. Int. Ed.* **2004**, *43*, 118 – 121; b) M. Valden, X. Lai, D. W. Goodman, *Science* **1998**, *281*, 1647 – 1650.

[4] a) Z. P. Liu, X. Q. Gong, J. Kohanoff, C. Sanchez, P. Hu, *Phys. Rev. Lett.* **2003**, *91*, 266102; b) V. Cooper, A. Kolpak, Y. Yourdshahyan, A. Rappe in *Nanotechnology in Catalysis* (Eds.: B. Zhou, S. Han, R. Raja, G. Somorjai), Springer, New York, **2007**, pp. 13 – 21; c) B. Yoon, H. Häkkinen, U. Landman, A. S. Wörz, J.-M. Antonietti, S. Abbet, K. Judai, U. Heiz, *Science* **2005**, *307*, 403 – 407.

[5] B. Hammer, J. K. Nørskov in *Advances in Catalysis*, *Vol. 45* (Ed.: H. Knozinger, B. C. Gates), Academic Press, New York, **2000**, pp. 71 – 129.

[6] a) L.-S. Wang, *Phys. Chem. Chem. Phys.* **2010**, *12*, 8694 – 8705; b) P. Pyykkö, *Angew. Chem.* **2004**, *116*, 4512 – 4557; *Angew. Chem. Int. Ed.* **2004**, *43*, 4412 – 4456.

[7] W. Liu, Y. F. Zhu, Q. Jiang, *J. Phys. Chem. C* **2010**, *114*, 21094 – 21099.

[8] a) M. Cargnello, C. Gentilini, T. Montini, E. Fonda, S. Mehraeen, M. Chi, M. Herrera-Collado, N. D. Browning, S. Polizzi, L. Pasquato, P. Fornasiero, *Chem. Mater.* **2010**, *22*, 4335 – 4345; b) H. Y. Kim, H. M. Lee, G. Henkelman, *J. Am. Chem. Soc.* **2012**, *134*, 1560 – 1570.

[9] N. J. Lawrence, J. R. Brewer, L. Wang, T.-S. Wu, J. M. Wells-Kingsbury, M. M. Ihrig, G. Wang, Y.-L. Soo, W.-N. Mei, C. L. Cheung, *Nano Lett.* **2011**, *11*, 2666 – 2671.

[10] P. Zhang, T. K. Sham, *Phys. Rev. Lett.* **2003**, *90*, 245502.

[11] Q. Fu, H. Saltsburg, M. Flytzani-Stephanopoulos, *Science* **2003**, *301*, 935 – 938.

[12] M. Škoda, M. Cabala, I. Matolinová, K. C. Prince, T. Skála, F. Šutara, K. Veltruská, V. Matolin, *J. Chem. Phys.* **2009**, *130*, 034703.

[13] R. Courths, H. G. Zimmer, A. Goldmann, H. Saalfeld, *Phys. Rev. B* **1986**, *34*, 3577 – 3585.

[14] Q.-H. Wu, A. Thissen, W. Jaegermann, M. Schüz, P. C. Schmidt, *Chem. Phys. Lett.* **2006**, *430*, 309 – 313.

[15] J. C. Fuggle, *J. Electron Spectrosc. Relat. Phenom.* **1980**, *21*, 275 – 281.

[16] S. Bulusu, X. Li, L.-S. Wang, X. C. Zeng, *Proc. Natl. Acad. Sci. USA* **2006**, *103*, 8326 – 8330.

[17] E. M. Fernández, J. M. Soler, I. L. Garzón, L. C. Balbás, *Phys. Rev. B* **2004**, *70*, 165403.

[18] X. Lin, N. Nilius, H. J. Freund, M. Walter, P. Frondelius, K. Honkala, H. Häkkinen, *Phys. Rev. Lett.* **2009**, *102*, 206801.

